Geochemical and metagenomic characterization of Jinata Onsen, a Proterozoic-analog hot spring, reveals novel microbial diversity including iron-tolerant phototrophs and thermophilic lithotrophs

Lewis M. Ward[1,2,3]*, Airi Idei[4], Mayuko Nakagawa[2,5], Yuichiro Ueno[2,5,6], Woodward W. Fischer[3], Shawn E. McGlynn[2]*

1. Department of Earth and Planetary Sciences, Harvard University, Cambridge, MA 02138 USA
2. Earth-Life Science Institute, Tokyo Institute of Technology, Meguro, Tokyo, 152-8550, Japan
3. Division of Geological and Planetary Sciences, California Institute of Technology, Pasadena, CA 91125 USA
4. Department of Biological Sciences, Tokyo Metropolitan University, Hachioji, Tokyo 192-0397, Japan
5. Department of Earth and Planetary Sciences, Tokyo Institute of Technology, Meguro, Tokyo, 152-8551, Japan
6. Department of Subsurface Geobiological Analysis and Research, Japan Agency for Marine-Earth Science and Technology, Natsushima-cho, Yokosuka 237-0061, Japan

Correspondence: lewis_ward@fas.harvard.edu or mcglynn@elsi.jp

Abstract

Hydrothermal systems, including terrestrial hot springs, contain diverse geochemical conditions that vary over short spatial scales due to progressive interaction between the reducing hydrothermal fluids, the oxygenated atmosphere, and in some cases seawater. At Jinata Onsen, on Shikinejima Island, Japan, an intertidal, anoxic, iron-rich hot spring mixes with the oxygenated atmosphere and seawater over short spatial scales, creating a diversity of chemical potentials and redox pairs over a distance ~10 m. We characterized the geochemical conditions along the outflow of Jinata Onsen as well as the microbial communities present in biofilms, mats, and mineral crusts along its traverse via 16S rDNA amplicon and genome-resolved shotgun metagenomic sequencing. The microbial community changed significantly downstream as temperatures and dissolved iron concentrations decreased and dissolved oxygen increased. Near the spring source, biomass is limited relative to downstream, and primary productivity may be fueled by oxidation of ferrous iron and molecular hydrogen by members of the Zetaproteobacteria and Aquificae. Downstream, the microbial community is dominated by oxygenic Cyanobacteria. Cyanobacteria are abundant and active even at ferrous iron concentrations of ~150 μM, which challenges the idea that iron toxicity limited cyanobacterial expansion in Precambrian oceans. Several novel lineages of Bacteria are also present at Jinata Onsen, including previously uncharacterized members of the Chloroflexi and Caldithrichaeota phyla, positioning Jinata Onsen as a valuable site for future characterization of these clades.

Importance

High temperatures and reducing conditions allow hot springs to support microbial communities that are very different from those found elsewhere on the surface of the Earth today; in some ways, these environments and the communities they support can be similar to environments that existed on the early Earth and that may exist on other planets. Here, we describe a novel hot spring system where hot, iron-rich but oxygen-poor water flows into the ocean, supporting a range of unique microbial communities. Metagenomic sequencing recovered many novel microbial lineages, including deep-branching and uniquely thermotolerant members

of known groups. Comparison of the biological communities in the upstream part of the hot spring, potentially supported by biological iron and hydrogen oxidizing metabolisms, to downstream microbial mats, supported by oxygenic photosynthesis, provides insight into the potential productivity of life during Proterozoic time and on other planets where oxygenic photosynthesis is not possible.

Introduction

A major theme of environmental microbiology has been the enumeration of microbial groups that are capable of exploiting diverse chemical potentials (i.e. chemical disequilibria) that occur in nature (e.g. 1-3). Hot springs, with their varied chemical compositions, provide reservoirs of novel microbial diversity, where environmental and geochemical conditions select for lineages and metabolisms distinct from other Earth-surface environments (e.g. 4-7). In addition to their value as sources of microbial diversity, hot springs also provide valuable test beds for understanding microbial community processes driven by different suites of metabolisms (e.g. 8)—this in turn allows these systems to serve as process analogs and to provide a window into biosphere function during early times in Earth history, for example when the O_2 content of surface waters was low or non-existent. In contrast to most surface ecosystems which are fueled almost entirely by oxygenic photosynthesis by plants, algae, and Cyanobacteria, hot spring microbial communities are commonly supported by lithotrophic or anoxygenic phototrophic organisms that derive energy and electrons for carbon fixation by oxidizing geologically sourced electron donors such as Fe^{2+}, sulfide, and molecular hydrogen (e.g. 9-11). These communities may therefore provide insight into the function of microbial communities on the early Earth or other planets, in which oxygenic photosynthesis may be absent or less significant and anoxygenic photosynthetic or lithotrophic metabolisms may play a larger role, resulting in overall lower rates of primary productivity (e.g. 12-15).

Here, we present a geomicrobiological characterization of a novel Precambrian Earth process analog site: Jinata Onsen, on Shikinejima Island, Tokyo Prefecture, Japan. At Jinata hot spring, anoxic, iron-rich hydrothermal fluids feed a subaerial spring that flows into a small bay, and mixes with seawater over the course of a few meters. Over its course the waters transition from low-oxygen, iron-rich conditions analogous to some aspects of the early Proterozoic oceans, toward iron-poor and oxygen-rich conditions typical of modern coastal oceans. In upstream regions of the stream where oxygenic Cyanobacteria are absent, biomass is visibly sparse; however, downstream, biomass accumulates in the form of thick microbial mats containing abundant Cyanobacteria. Visible differences in accumulation and appearance of biomass across the temperature and redox gradient establish the hypothesis that microbial community composition, as well as magnitude and metabolic drivers of primary productivity, varies along the spring flow. To begin testing this hypothesis and to provide a baseline description of the geochemistry and microbiology of this site in support of future investigation, we performed geochemical measurements, 16S rDNA amplicon sequencing, and genome-resolved metagenomic sequencing to recover draft genomes of diverse novel microbial lineages that inhabit Jinata Onsen.

Results

Site description

The source water of Jinata Onsen emerges with dissolved oxygen concentrations below our limit of detection, is iron-rich, and gently bubbles gas from the spring source (Table 1,

Figure 1, Figure 2). Temperatures at the source are ~63°C. Water emerges into the Source Pool, which has no visible microbial mats or biofilms (Figure 2D). Surfaces are instead coated with a fluffy red precipitate, likely a poorly ordered or short range-ordered ferric iron oxide phase such as ferrihydrite. Flow from the source is—at least in part—tidally charged, with the highest water levels and flow rates occurring at high tide. At low tide, flow rates drop and the water level of the Source Pool can drop by decimeters and portions of the Source Pool can drain during spring low tides. Downstream, the spring water collects into a series of pools (Pool 1-3) (Figure 2C,E-F), which cool sequentially (Figure 3, Supplemental Table 1). Pool 1 contains iron oxides like the Source Pool, but also develops macroscopic microbial streamers that are coated in iron oxides and thin veil-like layers of microorganisms overlaying iron oxide sediments—structures similar to those typically made by marine iron-oxidizing Zetaproteobacteria (e.g. 16). Streamers are very fine (mm-scale) and delicate (break apart on contact with forceps) but can reach several centimeters in length. Cyanobacteria in Pool 2 and Pool 3 display high levels of photosynthetic activity as revealed by high dissolved oxygen concentration (~234 µM), low dissolved inorganic carbon concentrations, and the accumulation of visible O_2 bubbles on the surface and within the fabric of the mat. Downstream pools (Pools 2 and 3) mix with seawater during high tide due to wave action, but this seawater influence does not appear to influence the Source Pool or Pool 1. Samples were collected and temperatures were measured at high tide, reflecting the lowest temperatures experienced by microbes in the pools—at low tide, hot spring input is dominant and temperatures rise (observed range at each site in Supplemental Table 1). Subaqueous surfaces in Pools 2 and 3 are covered in thick microbial mats. In Pool 2, the mat is coated in a layer of fluffy iron oxide similar to that in the Source Pool, with dense microbial mat below (Figure 2E). Pool 3 contains only patchy iron oxides, with mostly exposed microbial mats displaying a finger-like morphology. These "fingers" were 0.5-1 cm in diameter and up to ~5 cm long and were closely packed and carpeting surfaces of Pool 3 below the high tide line, potentially related to turbulent mixing from wave action during high tide (Figure 2F). The Outflow is the outlet of a channel connecting Pool 2 to the bay. Its hydrology is dominantly marine with small admixtures of inflowing spring water (Figure 2G).

Geochemistry

Geochemical measurements along the flow path of Jinata Onsen revealed a significant shift from hot, low-oxygen, high-iron source water to cooler, more oxygen-rich water with less dissolved iron downstream. Geochemistry measurements of Jinata source water are summarized in Table 1 and Supplemental Table 1, while geochemical gradients along the stream outflow are summarized in Figure 3 and Supplemental Table 2. Source waters were slightly enriched in chloride relative to seawater (~23.2 g/L in Jinata source water versus ~19.4 g/L in typical seawater), depleted in sulfate (~1.6 g/L in Jinata versus ~2.7 g/L in seawater) but approached seawater concentrations downstream as mixing increased. Water emerging from the source was 63°C, very low in dissolved oxygen (~4.7 µM), at pH 5.4, and contained substantial concentrations of dissolved iron (~250 µM Fe^{2+}). Dissolved organic carbon (DOC) in the source water was high (~1.31 mM). It is unknown whether this is produced *in situ* or whether the source water emerges with high DOC. Both DOC and DIC decrease along the outflow of the spring (Supplemental Table 1). After emerging from the source, the spring water exchanges gases with the air due to mixing associated with water flow and gas ebullition, and DO rose to 39 µM at the surface of the Source Pool. As water flows downstream from the Source Pool, it cools slightly, exchanges gases with the atmosphere, and intermittently mixes with seawater below Pool 1.

16S rDNA and genome-resolved metagenomic sequencing

16S rDNA and metagenomic sequencing of microbial communities at Jinata Onsen revealed a highly diverse community. In total, 16S rDNA amplicon sequencing recovered 456,737 sequences from the 10 samples at Jinata (Supplemental Tables 3-5). Reads per sample ranged from 26,057 Source Pool Sample A to 97,445 for Pool 1 Sample A (median 43,331, mean 45,673, and standard deviation 19,568). On average 74% of the microbial community was recovered from Jinata samples at the 99% OTU level based on the Good's Coverage statistic of the 16S rRNA gene (ranging from 54% coverage in the Outflow Sample A to 85% in the Pool 1 Sample A) and 87% at the 97% OTU level (74% for the Outflow Sample A to 94.5% for the Pool 1 Sample B). The incomplete sampling—despite sequencing to relatively high depth (>26000 reads per sample)—probably reflects uneven diversity. Greater than 50% of the reads observed at most sites map to the 10 most abundant taxa (Supplemental Table 4). MDS analysis (Supplemental Figure 1) demonstrates that samples from the same site are highly similar, and adjacent sites (e.g. Source Pool and Pool 1, Outflow and Pool 3) show significant similarity. However, there is a significant transition in microbial community diversity between the most distant samples (e.g. Source Pool and Outflow).

Shotgun metagenomic sequencing of four samples from Jinata Onsen recovered 121 GB of data, forming a 1.48 Gb coassembly consisting of 1531443 contigs with an N50 of 1494 bp. Nucleotide composition and differential coverage-based binning of the coassembly via multiple methods followed by dereplication and refinement resulted in a final set of 161 medium- or high-quality metagenome-assembled genomes (MAGs) following current standards (i.e. completeness >50% and contamination <10%) (17). These MAGs are from diverse phyla of Bacteria and Archaea (Figure 4); metagenome and MAG statistics with tentative taxonomic assignments for recovered MAGs are available in Supplementary Table 5, while MAGs of particular interest are discussed in depth below and in the SI and shown in phylogenetic trees alongside reference strains in Figures 5-7.

Discussion

As Jinata spring water flows from source to ocean, it transitions from hot, low-oxygen, high-iron water to cooler, iron-depleted, oxygen-rich water in downstream regions (Figure 3). Following this geochemical transition is a major shift in the composition of the microbial community, from a high-temperature, putatively lithotrophic community which produces little visible biomass upstream, to a lower temperature, community with well-developed, thick microbial mats downstream. This shift in community composition is summarized in Figure 3, with complete diversity data in the Supplemental Information (including OTU counts per samples in Supplemental Table 4 and relative abundance binned at the class level in Supplemental Table 5). Below, we discuss the overall physiological and taxonomic trends across the spring sites as inferred from diversity and genomic analysis.

Potential for iron and hydrogen oxidation

The hot spring water emerging at the Source Pool at Jinata contains abundant electron donors including dissolved Fe^{2+} and likely H_2 (though measurements of gas content varied, as discussed in the SI) (Table 1). Although rates of carbon fixation were not measured, the appearance of zetaproteobacterial veils and streamers and molecular evidence for lithoautotrophic microbes suggests that these electron donors may fuel productivity and determine the microbial community upstream at the Source Pool and Pool 1, where microbial mats are not well developed. The low accumulation of biomass in upstream regions of Jinata are similar to other microbial ecosystems fueled by iron oxidation (e.g. Oku-Okuhachikurou Onsen,

11, Fuschna Spring, 18, and Jackson Creek, 19), in which lithotrophic communities appear capable of accumulating less organic carbon than communities fueled by oxygenic photosynthesis (including those in downstream regions at Jinata).

Results of 16S rDNA sequencing indicate that the most abundant organisms in the Source Pool are members of the Aquificae family Hydrogenothermaceae (33% of reads in the Source Pool and 11.6% of reads in Pool 1). Members of this family of marine thermophilic lithotrophs are capable of iron and hydrogen oxidation, as well as heterotrophy (20) and may be utilizing either Fe^{2+} or H_2 at Jinata. The seventh most abundant OTU in the Source Pool samples is a novel sequence 89% similar to a strain of *Persephonella* found in an alkaline hot spring in Papua New Guinea. *Persephonella* is a genus of thermophilic, microaerophilic hydrogen oxidizing bacteria within the Hydrogenothermaceae (21). Despite their abundance as assessed by 16S rDNA sequencing (Figure 3), only four partial Aquificae MAGs were recovered from Jinata of which only one (J026) was reasonably complete (~94%). Two Aquificae MAGs recovered Group 1 NiFe hydrogenase genes, which may be used in hydrogenotrophy; the absence of hydrogenases from the other MAGs may be related to their low completeness, or could reflect a utilization of iron or other electron donors and not H_2 in these organisms.

The other most abundant organisms near the source are members of the Zetaproteobacteria—a group typified by the neutrophilic, aerobic iron-oxidizing genus *Mariprofundus* common in marine systems (22). Zetaproteobacteria accounted for 24.5% of 16S rDNA sequences in the Source Pool and 26.7% in Pool 1. All Zetaproteobacteria characterized to date are obligate iron- and/or hydrogen-oxidizing lithoautotrophs (23), suggesting that these organisms may play a substantial role in driving carbon fixation in the Source Pool and Pool 1.

Members of the Mariprofundaceae have been observed to have an upper temperature limit for growth of 30 °C (24), while Zetaproteobacteria are found at Jinata at temperatures up to 63 °C. This currently represents a unique high-temperature environment for these organisms. In particular, the third most abundant OTU in the Source Pool and Pool 1 sample A is an unknown sequence that is 92% identical to a sequence from an uncultured zetaproteobacterium from a shallow hydrothermal vent in Papua New Guinea (25). This sequence likely marks a novel lineage of high-temperature iron-oxidizing Zetaproteobacteria. Four MAGs affiliated with the Zetaproteobacteria were recovered from Jinata with completeness estimates by CheckM ranging from ~80 to ~97% (J005, J009, J030, and J098). While these MAGs did not recover 16S rRNA genes, RpoB- and concatenated ribosomal protein-based phylogenies illustrated that members of this group at Jinata Onsen do not belong to the characterized genera *Mariprofundus* or *Ghiorsea*, but instead form separate basal lineages within the Zetaproteobacteria (Figure 5). Despite their phylogenetic distinctness, these MAGs largely recovered genes associated with aerobic iron oxidation as expected given the physiology of other Zetaproteobacteria, including Cyc2 cytochrome and C-family heme copper oxidoreductase genes (SI). Notable exceptions are J005 and J030 which did not recover genes for carbon fixation via the Calvin cycle (such as the large and small subunits of rubisco, phosphoribulose kinase, or carboxysome proteins); the high completeness of these MAGs (~94-97%) makes it unlikely that these genes would all fail to be recovered (MetaPOAP False Negative estimates 10^{-5}-10^{-7}); the absence of carbon fixation pathways from these genomes together with the availability of abundant dissolved organic carbon in Pool 1 (~1.3 mM) suggest that these organisms may be heterotrophic, a lifestyle not previously observed for members of the Zetaproteobacteria.

Seven MAGs were recovered from the enigmatic bacterial phylum Calditrichaeota (J004, J008, J042, and J075) (Figure 6). While few members of Calditrichaeota have been isolated or sequenced, the best known of these is *Caldithrix abyssi* (26); this taxon was characterized as an anaerobic thermophile capable of lithoheterotrophic H_2 oxidation coupled to denitrification and organoheterotrophic fermentation (27, 28). The Calditrichaeota MAGs reported here are up to 97% complete (J004) and contain members with variable putative metabolic capabilities, potentially including aerobic hydrogen- or iron-oxidizing lithoautotrophy (SI). Unlike previously described Calditrichaeota which are all heterotrophic (28), most of the Calditrichaeota MAGs reported here possess a putative capacity for carbon fixation via the Calvin cycle. J004 is closely related to *Caldithrix abyssi*, while the other MAGs form two distinct but related clades (Figure 6).

Oxygenic photosynthesis

Cyanobacteria are nearly absent from near the Source Pool, but are observed in low numbers in Pool 1 and become dominant starting in Pool 2. The most abundant Cyanobacteria present are predominantly members of Subsection III, Family I. This group includes *Leptolyngbya*, a genus of filamentous non–heterocystous Cyanobacteria that is present in other hot springs of similar temperatures (e.g. 11, 29, 30). Diverse cyanobacterial MAGs were recovered, including members of the orders Pleurocapsales (J083), Chroococcales (J003 and J149), and Oscillatoriales (J007, J055, and J069). In the Outflow samples, chloroplast sequences are abundant, most closely related to the diatom *Melosira*.

Cyanobacteria are sometimes underrepresented in iTag datasets as a result of poor DNA yield or amplification biases (e.g. 31, 32), but the low abundance of Cyanobacteria near the Source Pool was confirmed by fluorescent microscopy, in which cells displaying cyanobacterial autofluorescence were observed abundantly in samples from the downstream samples but not in the Source Pool (Supplemental Figure 2). Thick microbial mats first appear in Pool 2 when Cyanobacteria become abundant, suggesting that oxygenic photosynthesis fuels more net carbon fixation than lithotrophy in these environments. Previously, it has been suggested that high ferrous iron concentrations are toxic to Cyanobacteria, and that this would have greatly reduced their productivity under ferruginous ocean conditions such as those that may have persisted through much of the Archean era (33). The abundant Cyanobacteria observed to be active at Jinata under high iron concentrations suggest that Cyanobacteria can adapt to ferruginous conditions, and therefore iron toxicity might not inhibit Cyanobacteria over geological timescales. Indeed, the soluble iron concentrations observed at Jinata are higher (150-250 μM) than predicted for the Archean oceans (<120 μM, 34) or observed at other iron-rich hot springs (~100-200 μM, 11, 35), making Jinata an excellent test case for determining the ability of Cyanobacteria to adapt to high iron concentrations. Culture-based physiological experiments may be useful to determine whether Jinata Cyanobacteria utilize similar strategies to other iron-tolerant strains (e.g. by those in Chocolate Pots Hot Spring, 35, or the ferric iron-tolerant *Leptolyngbya*-relative *Marsacia ferruginose*, 36) or whether Jinata strains possess unique adaptations that allow them to grow at higher iron concentrations than known for other environmental Cyanobacteria strains. This will in turn provide insight into whether iron tolerance is due to evolutionarily conserved strategies or whether this is a trait that has evolved convergently multiple times.

Diverse novel Chloroflexi from Jinata Onsen

In addition to the primary phototrophic and lithotrophic carbon fixers at Jinata, 16S rDNA and metagenomic data sets revealed diverse novel lineages within the Chloroflexi phylum.

A total of 23 Chloroflexi MAGs were recovered, introducing substantial genetic and metabolic diversity that expands our understanding of this group. While the best known members of this phylum are Type 2 Reaction Center-containing lineages such as *Chloroflexus* and *Roseiflexus* within the class Chloroflexia (e.g. 37), phototrophy is not a synapomorphy of the Chloroflexi phylum or even the Chloroflexia class (e.g. 38) and most of the diversity of the phylum belongs to several other classes made up primarily of nonphototrophic lineages (7). The bulk of Chloroflexi diversity recovered from Jinata belongs to "subphlyum I", a broad group of predominantly nonphototrophic lineages that was originally described based on the classes Anaerolineae and Caldilineae (39), but also encompasses the related classes Ardenticatenia, Thermoflexia, and *Candidatus* Thermofonsia (7, 40, 41).

16S rDNA analysis indicates that members of the Chloroflexi class Anaerolineae are common throughout Jinata with the exception of the Outflow (average 3.5% relative abundance). However, it is likely that a large fraction of 16S rDNA sequences annotated as Anaerolineae at Jinata Onsen belong to the sister class *Candidatus* Thermofonsia (7). Three MAGs recovered from Jinata (J082, J097, and J130) are associated with the Anaerolineae class as determined by RpoB and concatenated ribosomal protein phylogenies, as compared to seven associated with *Ca.* Thermofonsia (J027, J033, J036, J038, J039, J064, and J076). Particularly notable among these MAGs is J036, a close relative of the phototrophic *Ca.* Roseilinea gracile (42-44). J036 contains a 16S rRNA gene that is 96% similar to that of *Ca*. Roseilinea gracile, and two-way AAI estimates (Rodriguez and Konstantinidis 2014) showed 73.6% similarity between the two strains, indicating these strains are probably best classified as distinct species within the same genus. Unlike other phototrophs in the Chloroflexi phylum that are capable of photoautotrophy via the 3-hydroxypropionate bicycle or the Calvin Cycle (45, 46), J036 and *Ca.* Roseilinea gracile do not encode carbon fixation and are likely photoheterotrophic.

Members of the Chloroflexi class Caldilineae were present at up to ~1% abundance at Jinata in the 16S rDNA dataset. Three MAGs were recovered that form a deeply branching lineage with the Caldilineae class (J095, J111, and J123), sister to the previously characterized genera *Caldilinea* and *Litorilinea*. Like other members of the Caldilineae, these strains encode aerobic respiration via A-family heme copper oxidoreductases and both a *bc* complex III and an alternative complex III, and are therefore likely at least facultatively aerobic. J095 also encodes carbon fixation via the Calvin cycle as well as a Group 1f NiFe hydrogenase, suggesting a potential capability for lithoautotrophy by hydrogen oxidation, expanding the known metabolic diversity of this class and the Chloroflexi phylum as a whole. MAG J114 branches at the base of subphylum I of the Chloroflexi, potentially the first member of a novel class-level lineage. The divergence between Anaerolineae and Caldilineae has been estimated to have occurred on the order of 1.7 billion years ago (46). The phylogenetic placement of J114 suggests that it diverged from other members of subphylum I even earlier, and it may be a good target for future investigation to assess aspects of the early evolution of the Chloroflexi phylum. J114 encodes genes that suggest the capacity for aerobic hydrogen-oxidizing autotrophy (including those encoding an A-family heme copper oxidoreductase, a Group 1f NiFe hydrogenase, and rubisco, SI) —a lifestyle not previously described for members of the Chloroflexi.

Conclusions

The diversity of iron oxidizing bacteria at Jinata is different than in other Fe^{2+} -rich springs and environments. For example, in freshwater systems such as Oku-Okuhachikurou Onsen in Akita Prefecture, Japan (11), and Budo Pond in Hiroshima, Japan (47), iron oxidation

is driven primarily by the activity of chemoautotrophs such as members of the Gallionellaceae. In contrast, at Chocolate Pots hot spring in Yellowstone National Park, USA, iron oxidation is primarily abiotic, driven by O_2 produced by Cyanobacteria, with only a small contribution from iron oxidizing bacteria (48, 49). The distinct iron-oxidizing community at Jinata Onsen may be related to the salinity of the spring water, or biogeographically by access to the ocean, as Zetaproteobacteria are typically found in marine settings, particularly in deep ocean basins associated with hydrothermal iron sources (24). Despite the taxonomically distinct iron oxidizer communities between Jinata and Oku-Okuhachikurou Onsen, both communities support only limited biomass in regions dominated by iron oxidizers (11), perhaps reflecting the shared biochemical and bioenergetic challenges iron oxidation incurred by diverse iron oxidizing bacteria including Gallionellaceae and Zetaproteobacteria (11, 24, 50). Future work focused on isolation and physiological characterization of microbes, quantification of rates and determination of microbial drivers of carbon fixation and aerobic and anaerobic heterotrophy, and carbon isotope profiling of organic and inorganic species along the flow path of the hot spring will be necessary to fully characterize the activity of microbes at Jinata and to fully compare this system to other areas with high dissolved ferrous iron concentrations (e.g. Oku-Okuhachikurou Onsen, 11, Fuschna Spring, 18, Jackson Creek, 19, and Chocolate Pots Hot Spring, 48, 49).

Throughout Earth history, the metabolic opportunities available to life, and the resulting organisms and metabolisms responsible for driving primary productivity, have been shaped by the geochemical conditions of the atmosphere and oceans. The modern, sulfate-rich, well-oxygenated oceans we see today reflect a relatively recent state—one typical of only the last few hundred million years (e.g. 51). For the first half of Earth history, until ~2.3 billion years ago (Ga), the atmosphere and oceans were anoxic (52), and the oceans were largely rich in dissolved iron but poor in sulfur (53). At this time, productivity was low and fueled by metabolisms such as methanogenesis and anoxygenic photosynthesis (12, 13, 15). Following the expansion of oxygenic photosynthesis by Cyanobacteria and higher primary productivity around the Great Oxygenation Event ~2.3 Ga (54-56), the atmosphere and surface ocean accumulated some oxygen, and the ocean transitioned into a state with oxygenated surface waters but often anoxic deeper waters, rich in either dissolved iron or sulfide (57-60). At Jinata Onsen, this range of geochemical conditions is recapitulated over just a few meters, providing a useful test case for probing the shifts of microbial productivity over the course of Earth history as conditions vary over short spatial scales. In particular, the concomitant increase in visible biomass at Jinata as the community shifts from lithotrophy toward water-oxidizing phototrophy (i.e. oxygenic photosynthesis) is consistent with estimates for greatly increased primary production following the evolution and expansion of Cyanobacteria around the GOE (14, 15, 55, 56).

The dynamic abundances of redox-active compounds including oxygen, iron, and hydrogen at Jinata may not only be analogous to conditions on the early Earth, but may have relevance for potentially habitable environments on Mars as well. Early Mars is thought to have supported environments with metabolic opportunities provided by the redox gradient between the oxidizing atmosphere and abundant electron donors such as ferrous iron and molecular hydrogen sourced from water/rock interactions (e.g. 61), and production of these substrates may continue today (62, 63). Understanding the potential productivity of microbial communities fueled by lithotrophic metabolisms is critical for setting expectations of the presence and size of potential biospheres on other worlds and early in Earth history (e.g. 11, 15). Uncovering the range of microbial metabolisms present under the environmental conditions at Jinata, and their

366 relative contributions to primary productivity, may therefore find application to predicting
367 environments on Mars most able to support productive microbial communities.
368
369 **Materials and Methods:**
370 **Geological context and sedimentology of Jinata:**
371 Jinata Onsen is located at 34.318 N, 139.216 E on the island of Shikinejima, Tokyo
372 Prefecture, Japan. Shikinejima is part of the Izu Islands, a chain of volcanic islands that formed
373 in the last few million years along the northern edge of the Izu-Bonin-Mariana Arc (64).
374 Shikinejima is formed of Late Paleopleistocene- to-Holocene non-alkaline felsic volcanics and
375 Late-Miocene to Pleistocene non-alkaline pyroclastic volcanic flows, with Jinata Onsen located
376 on a small bay on the southern side of the island (Figure 1).
377 **Sample collections:**
378 Five sites were sampled at Jinata Onsen: the Source Pool, Pool 1, Pool 2, Pool 3, and the
379 Outflow (Figure 1, Figure 2). During the first sampling trip in January 2016, two whole
380 community DNA samples were collected from each site for 16S rDNA amplicon sequencing.
381 During the second sampling trip, additional DNA was collected from the Source Pool and Pool 2
382 for shotgun metagenomic sequencing along with gas samples for qualitative analysis. Samples
383 for quantitative gas analysis were collected in October 2017 and April 2018.
384 Samples were collected as mineral scrapings of loosely attached, fluffy iron oxide coating
385 from surfaces and clasts upstream (Source Pool and Pool 1) and as samples of microbial mat
386 downstream (Pools 2 and 3, and Outflow) using sterile forceps and spatulas (~0.25 cm^3 of
387 material). Immediately after sampling, cells were lysed and DNA preserved with a Zymo
388 Terralyzer BashingBead Matrix and Xpedition Lysis Buffer. Lysis was achieved by attaching
389 tubes to the blade of a cordless reciprocating saw (Black & Decker, Towson, MD) and operating
390 for 1 minute. Aqueous geochemistry samples consisted of water collected with sterile syringes
391 and filtered through a 0.2 µm filter. Gas samples were collected near sites of ebullition emerging
392 from the bottom of the Source Pool; collection was done into serum vials by water substitution,
393 and then sealed underwater to prevent contamination by air.
394 **Geochemical analysis:**
395 Dissolved oxygen (DO), pH, and temperature measurements were performed *in situ* using
396 an Extech DO700 8-in-1 Portable Dissolved Oxygen Meter (FLIR Commercial Systems, Inc.,
397 Nashua, NH). Iron concentrations were measured using the ferrozine assay (65) following
398 acidification with 40 mM sulfamic acid to inhibit iron oxidation by O_2 or oxidized nitrogen
399 species (66). Ammonia/ammonium concentrations were measured using a TetraTest NH_3/NH_4^+
400 Kit (TetraPond, Blacksburg, VA) following manufacturer's instructions but with colorimetry of
401 samples and NH_4Cl standards quantified with a Thermo Scientific Nanodrop 2000c
402 spectrophotometer (Thermo Fisher Scientific, Waltham, MA) at 700 nm to improve sensitivity
403 and accuracy. Anion concentrations were measured via ion chromatography on a Shimadzu Ion
404 Chromatograph (Shimadzu Corp., Kyoto, JP) equipped with a Shodex SI-90 4E anion column
405 (Showa Denko, Tokyo, JP).
406 Presence of H_2 and CH_4 in gas samples was qualitatively determined with a Shimadzu
407 GC-14A gas chromatograph within 12 hours of collection to minimize oxidation of reduced
408 gases. Quantitative gas composition was measured following methods described in Suda et al.
409 2017 (67) and in the SI.
410 **16S rDNA and metagenomic sequencing and analysis:**

Sequencing of 16S rDNA followed methods described previously (11) and detailed in the SI. Following initial characterization via 16S rDNA sequencing, four samples were selected for shotgun metagenomic sequencing: JP1-A and JP3-A from the first sampling trip, and JP1L-1 and JP2-1 from the second sampling trip. Purified DNA was submitted to SeqMatic LLC (Fremont, CA) for library preparation and 2x100bp paired-end sequencing via Illumina HiSeq 4000 technology. Samples JP1-A and JP3-A shared a single lane with two samples from another project (7), while JP1L-1 and JP2-1 shared a lane with one sample from another project.

Raw sequence reads from all four samples were co-assembled with MegaHit v. 1.02 (68) and genome bins constructed based on nucleotide composition and differential coverage using MetaBAT (69), MaxBin (70), and CONCOCT (71) prior to dereplication and refinement with DAS Tool (72) to produce the final bin set. Genome bins were assessed for completeness, contamination, and strain-level heterogeneity using CheckM (73), tRNA sequences found with Aragorn (74), and presence of metabolic pathways of interest predicted with MetaPOAP (75). Coverage was extracted using bbmap (76) and samtools (77). Genes of interest (e.g. coding for ribosomal, photosynthesis, iron oxidation, and electron transport proteins) were identified from assembled metagenomic data locally with BLAST+ (78) and were screened against outlier (e.g. likely contaminant) contigs as determined by CheckM using tetranucleotide, GC, and coding density content. Translated protein sequences of genes of interest were aligned with MUSCLE (79), and alignments manually curated in Jalview (80). Phylogenetic trees were calculated using RAxML (81) on the Cipres science gateway (82). Node support for phylogenies was calculated with transfer bootstraps by BOOSTER (83). Trees were visualized with the Interactive Tree of Life viewer (84). Because sequencing depth of each sample in the full metagenome was uneven, relative abundance of genes of interest between metagenomic datasets was normalized to the coverage of *rpoB* genes in each raw dataset as mapped onto the coassembly. Like the 16S rRNA gene, *rpoB* is a highly conserved, vertically-inherited gene useful for taxonomic identification of organisms but has the added advantage that it is only known to occur as a single copy per genome (85) and is more readily assembled in metagenomic datasets (e.g. 7). Presence and classification of hydrogenase genes was determined with HydDB (86). Taxonomic assignment of MAGs was made based on placement in a reference phylogeny built with concatenated ribosomal protein sequences following (87) and confirmed using GTDB-Tk (88).

Data availability:

Raw 16S rDNA, raw metagenomic sequence data, and MAGs have been uploaded and made publicly available on NCBI under Project Number PRJNA392119 (genome accession numbers can be found in Supplemental Table 6).

References

1. Broda, E., 1977. Two kinds of lithotrophs missing in nature. *Zeitschrift für allgemeine Mikrobiologie*, *17*(6), pp.491-493.
2. Ehrenreich, A. and Widdel, F., 1994. Anaerobic oxidation of ferrous iron by purple bacteria, a new type of phototrophic metabolism. *Applied and environmental microbiology*, *60*(12), pp.4517-4526.
3. Strous, M., Fuerst, J.A., Kramer, E.H., Logemann, S., Muyzer, G., van de Pas-Schoonen, K.T., Webb, R., Kuenen, J.G. and Jetten, M.S., 1999. Missing lithotroph identified as new planctomycete. *Nature*, *400*(6743), p.446.

4. Bryant, D.A., Costas, A.M.G., Maresca, J.A., Chew, A.G.M., Klatt, C.G., Bateson, M.M., Tallon, L.J., Hostetler, J., Nelson, W.C., Heidelberg, J.F. and Ward, D.M., 2007. Candidatus Chloracidobacterium thermophilum: an aerobic phototrophic acidobacterium. *Science*, *317*(5837), pp.523-526.
5. Eloe-Fadrosh, E.A., Paez-Espino, D., Jarett, J., Dunfield, P.F., Hedlund, B.P., Dekas, A.E., Grasby, S.E., Brady, A.L., Dong, H., Briggs, B.R. and Li, W.J., 2016. Global metagenomic survey reveals a new bacterial candidate phylum in geothermal springs. *Nature communications*, *7*, p.10476.
6. Beam, J.P., Jay, Z.J., Schmid, M.C., Rusch, D.B., Romine, M.F., de M Jennings, R., Kozubal, M.A., Tringe, S.G., Wagner, M. and Inskeep, W.P., 2016. Ecophysiology of an uncultivated lineage of Aigarchaeota from an oxic, hot spring filamentous 'streamer'community. *The ISME journal*, *10*(1), p.210.
7. Ward, L.M., Hemp, J., Shih, P.M., McGlynn, S.E. and Fischer, W.W., 2018. Evolution of phototrophy in the Chloroflexi phylum driven by horizontal gene transfer. *Frontiers in microbiology*, *9*, p.260.
8. Inskeep, W.P., Ackerman, G.G., Taylor, W.P., Kozubal, M., Korf, S. and Macur, R.E., 2005. On the energetics of chemolithotrophy in nonequilibrium systems: case studies of geothermal springs in Yellowstone National Park. *Geobiology*, *3*(4), pp.297-317.
9. Kawasumi, T., Igarashi, Y., Kodama, T. and Minoda, Y., 1980. Isolation of strictly thermophilic and obligately autotrophic hydrogen bacteria. *Agricultural and Biological Chemistry*, *44*(8), pp.1985-1986.
10. Spear, J.R., Walker, J.J., McCollom, T.M. and Pace, N.R., 2005. Hydrogen and bioenergetics in the Yellowstone geothermal ecosystem. *Proceedings of the National Academy of Sciences*, *102*(7), pp.2555-2560.
11. Ward, L.M., Idei, A., Terajima, S., Kakegawa, T., Fischer, W.W. and McGlynn, S.E., 2017. Microbial diversity and iron oxidation at Okuoku□hachikurou Onsen, a Japanese hot spring analog of Precambrian iron formations. *Geobiology*, *15*(6), pp.817-835.
12. Kharecha, P., Kasting, J. and Siefert, J., 2005. A coupled atmosphere–ecosystem model of the early Archean Earth. *Geobiology*, *3*(2), pp.53-76.
13. Canfield, D.E., Rosing, M.T. and Bjerrum, C., 2006. Early anaerobic metabolisms. *Philosophical Transactions of the Royal Society of London B: Biological Sciences*, *361*(1474), pp.1819-1836.
14. Sleep, N.H. and Bird, D.K., 2007. Niches of the pre□photosynthetic biosphere and geologic preservation of Earth's earliest ecology. *Geobiology*, *5*(2), pp.101-117.
15. Ward, LM, B Rasmussen, WW Fischer. 2018. Primary Productivity was Limited by Electron Donors Prior to the Advent of Oxygenic Photosynthesis. JGR Biogeosciences, in press.
16. Fullerton, H., Hager, K.W., McAllister, S.M. and Moyer, C.L., 2017. Hidden diversity revealed by genome-resolved metagenomics of iron-oxidizing microbial mats from Lō'ihi Seamount, Hawai'i. *The ISME journal*, *11*(8), p.1900.
17. Bowers, R.M., Kyrpides, N.C., Stepanauskas, R., Harmon-Smith, M., Doud, D., Reddy, T.B.K., Schulz, F., Jarett, J., Rivers, A.R., Eloe-Fadrosh, E.A. and Tringe, S.G., 2017. Minimum information about a single amplified genome (MISAG) and a metagenome-assembled genome (MIMAG) of bacteria and archaea. *Nature biotechnology*, *35*(8), p.725.
18. Hegler, F., Lösekann-Behrens, T., Hanselmann, K., Behrens, S. and Kappler, A., 2012. Influence of seasonal and geochemical changes on iron geomicrobiology of an iron-carbonate mineral water spring. *Applied and environmental microbiology*, pp.AEM-01440.

19. Roden, E., McBeth, J.M., Blothe, M., Percak-Dennett, E.M., Fleming, E.J., Holyoke, R.R., Luther III, G.W. and Emerson, D., 2012. The microbial ferrous wheel in a neutral pH groundwater seep. *Frontiers in Microbiology*, *3*, p.172.
20. Takai, K. and Nakagawa, S., 2014. The Family Hydrogenothermaceae. In *The Prokaryotes* (pp. 689-699). Springer, Berlin, Heidelberg.
21. Götz, D., Banta, A., Beveridge, T.J., Rushdi, A.I., Simoneit, B.R.T. and Reysenbach, A.L., 2002. Persephonella marina gen. nov., sp. nov. and Persephonella guaymasensis sp. nov., two novel, thermophilic, hydrogen-oxidizing microaerophiles from deep-sea hydrothermal vents. *International Journal of Systematic and Evolutionary Microbiology*, *52*(4), pp.1349-1359.
22. Emerson, D., Rentz, J.A., Lilburn, T.G., Davis, R.E., Aldrich, H., Chan, C. and Moyer, C.L., 2007. A novel lineage of proteobacteria involved in formation of marine Fe-oxidizing microbial mat communities. *PloS one*, *2*(8), p.e667.
23. Mori, J.F., Scott, J.J., Hager, K.W., Moyer, C.L., Küsel, K. and Emerson, D., 2017. Physiological and ecological implications of an iron-or hydrogen-oxidizing member of the Zetaproteobacteria, Ghiorsea bivora, gen. nov., sp. nov. *The ISME journal*, *11*(11), p.2624.
24. Emerson, D., Fleming, E.J. and McBeth, J.M., 2010. Iron-oxidizing bacteria: an environmental and genomic perspective. *Annual review of microbiology*, *64*, pp.561-583.
25. Meyer-Dombard, D., Amend, J.P. and Osburn, M.R., 2013. Microbial diversity and potential for arsenic and iron biogeochemical cycling at an arsenic rich, shallow-sea hydrothermal vent (Tutum Bay, Papua New Guinea). *Chemical Geology*, *348*, pp.37-47.
26. Miroshnichenko, M.L., Kostrikina, N.A., Chernyh, N.A., Pimenov, N.V., Tourova, T.P., Antipov, A.N., Spring, S., Stackebrandt, E. and Bonch-Osmolovskaya, E.A., 2003. Caldithrix abyssi gen. nov., sp. nov., a nitrate-reducing, thermophilic, anaerobic bacterium isolated from a Mid-Atlantic Ridge hydrothermal vent, represents a novel bacterial lineage. *International journal of systematic and evolutionary microbiology*, *53*(1), pp.323-329.
27. Alauzet, C. and Jumas-Bilak, E., 2014. The phylum Deferribacteres and the genus Caldithrix. In *The prokaryotes*(pp. 595-611). Springer, Berlin, Heidelberg.
28. Marshall, I.P., Starnawski, P., Cupit, C., Fernández Cáceres, E., Ettema, T.J., Schramm, A. and Kjeldsen, K.U., 2017. The novel bacterial phylum Calditrichaeota is diverse, widespread and abundant in marine sediments and has the capacity to degrade detrital proteins. *Environmental microbiology reports*, *9*(4), pp.397-403.
29. Roeselers, G., Norris, T.B., Castenholz, R.W., Rysgaard, S., Glud, R.N., Kühl, M. and Muyzer, G., 2007. Diversity of phototrophic bacteria in microbial mats from Arctic hot springs (Greenland). *Environmental Microbiology*, *9*(1), pp.26-38.
30. Bosak, T., Liang, B., Wu, T.D., Templer, S.P., Evans, A., Vali, H., Guerquin□Kern, J.L., Klepac□Ceraj, V., Sim, M.S. and Mui, J., 2012. Cyanobacterial diversity and activity in modern conical microbialites. *Geobiology*, *10*(5), pp.384-401.
31. Parada, A.E., Needham, D.M. and Fuhrman, J.A., 2016. Every base matters: assessing small subunit rRNA primers for marine microbiomes with mock communities, time series and global field samples. *Environmental microbiology*, *18*(5), pp.1403-1414.
32. Trembath-Reichert, E., Ward, L.M., Slotznick, S.P., Bachtel, S.L., Kerans, C., Grotzinger, J.P. and Fischer, W.W., 2016. Gene Sequencing-Based Analysis of Microbial-Mat Morphotypes, Caicos Platform, British West Indies. *Journal of Sedimentary Research*, *86*(6), pp.629-636.

33. Swanner, E.D., Mloszewska, A.M., Cirpka, O.A., Schoenberg, R., Konhauser, K.O. and Kappler, A., 2015. Modulation of oxygen production in Archaean oceans by episodes of Fe (II) toxicity. *Nature Geoscience*, *8*(2), pp.126-130.
34. Holland, H.D., 1984. *The chemical evolution of the atmosphere and oceans*. Princeton University Press.
35. Pierson, B.K., Parenteau, M.N. and Griffin, B.M., 1999. Phototrophs in high-iron-concentration microbial mats: physiological ecology of phototrophs in an iron-depositing hot spring. *Applied and environmental microbiology*, *65*(12), pp.5474-5483.
36. Brown, I.I., Bryant, D.A., Casamatta, D., Thomas-Keprta, K.L., Sarkisova, S.A., Shen, G., Graham, J.E., Boyd, E.S., Peters, J.W., Garrison, D.H. and McKay, D.S., 2010. Polyphasic characterization of a thermotolerant siderophilic filamentous cyanobacterium that produces intracellular iron deposits. *Applied and environmental microbiology*, *76*(19), pp.6664-6672.
37. Thiel, V., Tank, M. and Bryant, D.A., 2018. Diversity of chlorophototrophic bacteria revealed in the omics era. *Annual Review of Plant Biology*, *69*, pp.21-49.
38. Ward, L.M., Hemp, J., Pace, L.A. and Fischer, W.W., 2015. Draft genome sequence of Herpetosiphon geysericola GC-42, a nonphototrophic member of the Chloroflexi class Chloroflexia. *Genome announcements*, *3*(6), pp.e01352-15.
39. Yamada, T. and Sekiguchi, Y., 2009. Cultivation of uncultured chloroflexi subphyla: significance and ecophysiology of formerly uncultured chloroflexi'subphylum i'with natural and biotechnological relevance. *Microbes and Environments*, *24*(3), pp.205-216.
40. Kawaichi, S., Ito, N., Kamikawa, R., Sugawara, T., Yoshida, T. and Sako, Y., 2013. Ardenticatena maritima gen. nov., sp. nov., a ferric iron-and nitrate-reducing bacterium of the phylum 'Chloroflexi'isolated from an iron-rich coastal hydrothermal field, and description of Ardenticatenia classis nov. *International journal of systematic and evolutionary microbiology*, *63*(8), pp.2992-3002.
41. Dodsworth, J.A., Gevorkian, J., Despujos, F., Cole, J.K., Murugapiran, S.K., Ming, H., Li, W.J., Zhang, G., Dohnalkova, A. and Hedlund, B.P., 2014. Thermoflexus hugenholtzii gen. nov., sp. nov., a thermophilic, microaerophilic, filamentous bacterium representing a novel class in the Chloroflexi, Thermoflexia classis nov., and description of Thermoflexaceae fam. nov. and Thermoflexales ord. nov. *International journal of systematic and evolutionary microbiology*, *64*(6), pp.2119-2127.
42. Klatt, C.G., Wood, J.M., Rusch, D.B., Bateson, M.M., Hamamura, N., Heidelberg, J.F., Grossman, A.R., Bhaya, D., Cohan, F.M., Kühl, M. and Bryant, D.A., 2011. Community ecology of hot spring cyanobacterial mats: predominant populations and their functional potential. *The ISME journal*, *5*(8), p.1262.
43. Tank, M., Thiel, V., Ward, D.M. and Bryant, D.A., 2017. A panoply of phototrophs: an overview of the thermophilic chlorophototrophs of the microbial mats of alkaline siliceous hot springs in Yellowstone National Park, WY, USA. In *Modern topics in the phototrophic prokaryotes* (pp. 87-137). Springer, Cham.
44. Thiel, V., Hügler, M., Ward, D.M. and Bryant, D.A., 2017. The dark side of the mushroom spring microbial mat: life in the shadow of chlorophototrophs. II. Metabolic functions of abundant community members predicted from metagenomic analyses. *Frontiers in microbiology*, *8*, p.943.
45. Klatt, C.G., Bryant, D.A. and Ward, D.M., 2007. Comparative genomics provides evidence for the 3□hydroxypropionate autotrophic pathway in filamentous anoxygenic phototrophic bacteria and in hot spring microbial mats. *Environmental microbiology*, *9*(8), pp.2067-2078.

46. Shih, P.M., Ward, L.M. and Fischer, W.W., 2017. Evolution of the 3-hydroxypropionate bicycle and recent transfer of anoxygenic photosynthesis into the Chloroflexi. *Proceedings of the National Academy of Sciences*, *114*(40), pp.10749-10754.
47. Kato, S., Kikuchi, S., Kashiwabara, T., Takahashi, Y., Suzuki, K., Itoh, T., Ohkuma, M. and Yamagishi, A., 2012. Prokaryotic abundance and community composition in a freshwater iron-rich microbial mat at circumneutral pH. *Geomicrobiology Journal*, *29*(10), pp.896-905.
48. Trouwborst, R.E., Johnston, A., Koch, G., Luther III, G.W. and Pierson, B.K., 2007. Biogeochemistry of Fe (II) oxidation in a photosynthetic microbial mat: implications for Precambrian Fe (II) oxidation. *Geochimica et Cosmochimica Acta*, *71*(19), pp.4629-4643.
49. Fortney, N.W., He, S., Converse, B.J., Boyd, E.S. and Roden, E.E., 2018. Investigating the Composition and Metabolic Potential of Microbial Communities in Chocolate Pots Hot Springs. *Frontiers in microbiology*, *9*.
50. Bird, L.J., Bonnefoy, V. and Newman, D.K., 2011. Bioenergetic challenges of microbial iron metabolisms. *Trends in microbiology*, *19*(7), pp.330-340.
51. Lyons, T.W., Reinhard, C.T. and Planavsky, N.J., 2014. The rise of oxygen in Earth's early ocean and atmosphere. *Nature*, *506*(7488), p.307.
52. Johnson, J.E., Gerpheide, A., Lamb, M.P. and Fischer, W.W., 2014. O2 constraints from Paleoproterozoic detrital pyrite and uraninite. *Bulletin*, *126*(5-6), pp.813-830.
53. Walker, J.C. and Brimblecombe, P., 1985. Iron and sulfur in the pre-biologic ocean. *Precambrian Research*, *28*(3-4), pp.205-222.
54. Fischer, W.W., Hemp, J. and Johnson, J.E., 2016. Evolution of oxygenic photosynthesis. *Annual Review of Earth and Planetary Sciences*, *44*, pp.647-683.
55. Ward, L.M., Kirschvink, J.L. and Fischer, W.W., 2016. Timescales of oxygenation following the evolution of oxygenic photosynthesis. *Origins of Life and Evolution of Biospheres*, *46*(1), pp.51-65.
56. Crockford, P.W., Hayles, J.A., Bao, H., Planavsky, N.J., Bekker, A., Fralick, P.W., Halverson, G.P., Bui, T.H., Peng, Y. and Wing, B.A., 2018. Triple oxygen isotope evidence for limited mid-Proterozoic primary productivity. *Nature*, *559*(7715), p.613.
57. Canfield, D.E., 1998. A new model for Proterozoic ocean chemistry. *Nature*, *396*(6710), p.450.
58. Poulton, S.W., Fralick, P.W. and Canfield, D.E., 2010. Spatial variability in oceanic redox structure 1.8 billion years ago. *Nature Geoscience*, *3*(7), p.486.
59. Johnston, D.T., Wolfe-Simon, F., Pearson, A. and Knoll, A.H., 2009. Anoxygenic photosynthesis modulated Proterozoic oxygen and sustained Earth's middle age. *Proceedings of the National Academy of Sciences*, *106*(40), pp.16925-16929.
60. Johnston, D.T., Poulton, S.W., Dehler, C., Porter, S., Husson, J., Canfield, D.E. and Knoll, A.H., 2010. An emerging picture of Neoproterozoic ocean chemistry: Insights from the Chuar Group, Grand Canyon, USA. *Earth and Planetary Science Letters*, *290*(1-2), pp.64-73.
61. Hurowitz, J.A., Fischer, W.W., Tosca, N.J. and Milliken, R.E., 2010. Origin of acidic surface waters and the evolution of atmospheric chemistry on early Mars. *Nature Geoscience*, *3*(5), p.323.
62. Stamenković, V., Ward, L.M., Mischna, M. and Fischer, W.W., 2018. O 2 solubility in Martian near-surface environments and implications for aerobic life. *Nature Geoscience*, p.1.
63. Dzaugis, M., Spivack, A.J. and D'Hondt, S., 2018. Radiolytic H2 Production in Martian Environments. *Astrobiology*, *18*(9), pp.1137-1146.

64. Kaneoka, I., Isshiki, N. and Zashu, S., 1970. K-Ar ages of the Izu-Bonin islands. *Geochemical Journal*, *4*(2), pp.53-60.
65. Stookey, L.L., 1970. Ferrozine---a new spectrophotometric reagent for iron. *Analytical chemistry*, *42*(7), pp.779-781.
66. Klueglein, N. and Kappler, A., 2013. Abiotic oxidation of Fe (II) by reactive nitrogen species in cultures of the nitrate□reducing Fe (II) oxidizer A cidovorax sp. BoFeN1–questioning the existence of enzymatic Fe (II) oxidation. *Geobiology*, *11*(2), pp.180-190.
67. Suda, K., Gilbert, A., Yamada, K., Yoshida, N. and Ueno, Y., 2017. Compound–and position–specific carbon isotopic signatures of abiogenic hydrocarbons from on–land serpentinite–hosted Hakuba Happo hot spring in Japan. *Geochimica et Cosmochimica Acta*, *206*, pp.201-215.
68. Li, D., Liu, C.M., Luo, R., Sadakane, K. and Lam, T.W., 2015. MEGAHIT: an ultra-fast single-node solution for large and complex metagenomics assembly via succinct de Bruijn graph. *Bioinformatics*, *31*(10), pp.1674-1676.
69. Kang, D.D., Froula, J., Egan, R. and Wang, Z., 2015. MetaBAT, an efficient tool for accurately reconstructing single genomes from complex microbial communities. *PeerJ*, *3*, p.e1165.
70. Wu, Y.W., Tang, Y.H., Tringe, S.G., Simmons, B.A. and Singer, S.W., 2014. MaxBin: an automated binning method to recover individual genomes from metagenomes using an expectation-maximization algorithm. *Microbiome*, *2*(1), p.26.
71. Alneberg, J., Bjarnason, B.S., de Bruijn, I., Schirmer, M., Quick, J., Ijaz, U.Z., Loman, N.J., Andersson, A.F. and Quince, C., 2013. CONCOCT: clustering contigs on coverage and composition. *arXiv preprint arXiv:1312.4038*.
72. Sieber, C.M., Probst, A.J., Sharrar, A., Thomas, B.C., Hess, M., Tringe, S.G. and Banfield, J.F., 2018. Recovery of genomes from metagenomes via a dereplication, aggregation and scoring strategy. *Nature microbiology*, p.1.
73. Parks, D.H., Imelfort, M., Skennerton, C.T., Hugenholtz, P. and Tyson, G.W., 2015. CheckM: assessing the quality of microbial genomes recovered from isolates, single cells, and metagenomes. *Genome research*, pp.gr-186072.
74. Laslett, D. and Canback, B., 2004. ARAGORN, a program to detect tRNA genes and tmRNA genes in nucleotide sequences. *Nucleic acids research*, *32*(1), pp.11-16.
75. Ward, L.M., Shih, P.M.,.and Fischer, W.W, 2018. MetaPOAP: Presence or Absence of Metabolic Pathways in Metagenome-Assembled Genomes. *Bioinformatics*.
76. Bushnell, B. "BBMap short read aligner." *University of California, Berkeley, California. URL http://sourceforge. net/projects/bbmap* (2016).
77. Li, H., Handsaker, B., Wysoker, A., Fennell, T., Ruan, J., Homer, N., Marth, G., Abecasis, G. and Durbin, R., 2009. The sequence alignment/map format and SAMtools. *Bioinformatics*, *25*(16), pp.2078-2079.
78. Camacho, C., Coulouris, G., Avagyan, V., Ma, N., Papadopoulos, J., Bealer, K. and Madden, T.L., 2009. BLAST+: architecture and applications. *BMC bioinformatics*, *10*(1), p.421.
79. Edgar, R.C., 2004. MUSCLE: multiple sequence alignment with high accuracy and high throughput. *Nucleic acids research*, *32*(5), pp.1792-1797.
80. Waterhouse, A.M., Procter, J.B., Martin, D.M., Clamp, M. and Barton, G.J., 2009. Jalview Version 2—a multiple sequence alignment editor and analysis workbench. *Bioinformatics*, *25*(9), pp.1189-1191.

81. Stamatakis, A., 2014. RAxML version 8: a tool for phylogenetic analysis and post-analysis of large phylogenies. *Bioinformatics*, *30*(9), pp.1312-1313.
82. Miller, M.A., Pfeiffer, W. and Schwartz, T., 2010, November. Creating the CIPRES Science Gateway for inference of large phylogenetic trees. In *Gateway Computing Environments Workshop (GCE), 2010* (pp. 1-8). Ieee.
83. Lemoine, F., Entfellner, J.B.D., Wilkinson, E., Correia, D., Felipe, M.D., Oliveira, T. and Gascuel, O., 2018. Renewing Felsenstein's phylogenetic bootstrap in the era of big data. *Nature*, *556*(7702), p.452.
84. Letunic, I. and Bork, P., 2016. Interactive tree of life (iTOL) v3: an online tool for the display and annotation of phylogenetic and other trees. *Nucleic acids research*, *44*(W1), pp.W242-W245.
85. Case, R.J., Boucher, Y., Dahllöf, I., Holmström, C., Doolittle, W.F. and Kjelleberg, S., 2007. Use of 16S rRNA and rpoB genes as molecular markers for microbial ecology studies. *Applied and environmental microbiology*, *73*(1), pp.278-288.
86. Søndergaard, D., Pedersen, C.N. and Greening, C., 2016. HydDB: a web tool for hydrogenase classification and analysis. *Scientific reports*, *6*, p.34212.
87. Hug, L.A., Baker, B.J., Anantharaman, K., Brown, C.T., Probst, A.J., Castelle, C.J., Butterfield, C.N., Hernsdorf, A.W., Amano, Y., Ise, K. and Suzuki, Y., 2016. A new view of the tree of life. *Nature microbiology*, *1*(5), p.16048.
88. Parks, D.H., Chuvochina, M., Waite, D.W., Rinke, C., Skarshewski, A., Chaumeil, P.A. and Hugenholtz, P., 2018. A standardized bacterial taxonomy based on genome phylogeny substantially revises the tree of life. *Nature biotechnology*.
89. Singer, E., Emerson, D., Webb, E.A., Barco, R.A., Kuenen, J.G., Nelson, W.C., Chan, C.S., Comolli, L.R., Ferriera, S., Johnson, J. and Heidelberg, J.F., 2011. Mariprofundus ferrooxydans PV-1 the first genome of a marine Fe (II) oxidizing Zetaproteobacterium. *PloS one*, *6*(9), p.e25386.
90. Makita, H., Tanaka, E., Mitsunobu, S., Miyazaki, M., Nunoura, T., Uematsu, K., Takaki, Y., Nishi, S., Shimamura, S. and Takai, K., 2017. Mariprofundus micogutta sp. nov., a novel iron-oxidizing zetaproteobacterium isolated from a deep-sea hydrothermal field at the Bayonnaise knoll of the Izu-Ogasawara arc, and a description of Mariprofundales ord. nov. and Zetaproteobacteria classis nov. *Archives of microbiology*, *199*(2), pp.335-346.
91. Kublanov, I.V., Sigalova, O.M., Gavrilov, S.N., Lebedinsky, A.V., Rinke, C., Kovaleva, O., Chernyh, N.A., Ivanova, N., Daum, C., Reddy, T.B.K. and Klenk, H.P., 2017. Genomic analysis of Caldithrix abyssi, the thermophilic anaerobic bacterium of the novel bacterial phylum Calditrichaeota. *Frontiers in microbiology*, *8*, p.195.
92. Chang, Y.J., Land, M., Hauser, L., Chertkov, O., Del Rio, T.G., Nolan, M., Copeland, A., Tice, H., Cheng, J.F., Lucas, S. and Han, C., 2011. Non-contiguous finished genome sequence and contextual data of the filamentous soil bacterium Ktedonobacter racemifer type strain (SOSP1-21 T). *Standards in genomic sciences*, *5*(1), p.97.
93. Kuznetsov, B.B., Ivanovsky, R.N., Keppen, O.I., Sukhacheva, M.V., Bumazhkin, B.K., Patutina, E.O., Beletsky, A.V., Mardanov, A.V., Baslerov, R.V., Panteleeva, A.N. and Kolganova, T.V., 2011. Draft genome sequence of the anoxygenic filamentous phototrophic bacterium Oscillochloris trichoides subsp. DG-6. *Journal of bacteriology*, *193*(1), pp.321-322.
94. Sorokin, D.Y., Lücker, S., Vejmelkova, D., Kostrikina, N.A., Kleerebezem, R., Rijpstra, W.I.C., Damsté, J.S.S., Le Paslier, D., Muyzer, G., Wagner, M. and Van Loosdrecht, M.C.,

2012. Nitrification expanded: discovery, physiology and genomics of a nitrite-oxidizing bacterium from the phylum Chloroflexi. *The ISME journal*, *6*(12), p.2245.

95. Kawaichi, S., Yoshida, T., Sako, Y. and Nakamura, R., 2015. Draft genome sequence of a heterotrophic facultative anaerobic thermophilic bacterium, Ardenticatena maritima strain 110ST. *Genome announcements*, *3*(5), pp.e01145-15.
96. Hedlund, B.P., Murugapiran, S.K., Huntemann, M., Clum, A., Pillay, M., Palaniappan, K., Varghese, N., Mikhailova, N., Stamatis, D., Reddy, T.B.K. and Ngan, C.Y., 2015. High-quality draft genome sequence of Kallotenue papyrolyticum JKG1T reveals broad heterotrophic capacity focused on carbohydrate and amino acid metabolism. *Genome announcements*, *3*(6), pp.e01410-15.
97. Hemp, J., Ward, L.M., Pace, L.A. and Fischer, W.W., 2015. Draft genome sequence of Levilinea saccharolytica KIBI-1, a member of the Chloroflexi class Anaerolineae. *Genome announcements*, *3*(6), pp.e01357-15.
98. Hemp, J., Ward, L.M., Pace, L.A. and Fischer, W.W., 2015. Draft genome sequence of Ornatilinea apprima P3M-1, an anaerobic member of the Chloroflexi class Anaerolineae. *Genome announcements*, *3*(6), pp.e01353-15.
99. Hemp, J., Ward, L.M., Pace, L.A. and Fischer, W.W., 2015. Draft genome sequence of Ardenticatena maritima 110S, a thermophilic nitrate-and iron-reducing member of the Chloroflexi class Ardenticatenia. *Genome announcements*, *3*(6), pp.e01347-15.
100. Pace, L.A., Hemp, J., Ward, L.M. and Fischer, W.W., 2015. Draft genome of Thermanaerothrix daxensis GNS-1, a thermophilic facultative anaerobe from the Chloroflexi class Anaerolineae. *Genome announcements*, *3*(6), pp.e01354-15.
101. Ward, L.M., Hemp, J., Pace, L.A. and Fischer, W.W., 2015. Draft genome sequence of Leptolinea tardivitalis YMTK-2, a mesophilic anaerobe from the Chloroflexi class Anaerolineae. *Genome announcements*, *3*(6), pp.e01356-15.
102. Ward, L.M., McGlynn, S.E. and Fischer, W.W., 2018. Draft Genome Sequence of a Divergent Anaerobic Member of the Chloroflexi Class Ardenticatenia from a Sulfidic Hot Spring. *Genome announcements*, *6*(25), pp.e00571-18.
103. Ward, L.M., McGlynn, S.E. and Fischer, W.W., 2018. Draft Genome Sequences of Two Basal Members of the Anaerolineae Class of Chloroflexi from a Sulfidic Hot Spring. *Genome announcements*, *6*(25), pp.e00570-18.
104. Grouzdev, D.S., Rysina, M.S., Bryantseva, I.A., Gorlenko, V.M. and Gaisin, V.A., 2018. Draft genome sequences of 'Candidatus Chloroploca asiatica'and 'Candidatus Viridilinea mediisalina', candidate representatives of the Chloroflexales order: phylogenetic and taxonomic implications. *Standards in genomic sciences*, *13*(1), p.24.
105. Dunfield, P.F., Tamas, I., Lee, K.C., Morgan, X.C., McDonald, I.R. and Stott, M.B., 2012. Electing a candidate: a speculative history of the bacterial phylum OP10. *Environmental microbiology*, *14*(12), pp.3069-3080.
106. Ward, L.M., McGlynn, S.E. and Fischer, W.W., 2017. Draft Genome Sequences of a Novel Lineage of Armatimonadetes Recovered from Japanese Hot Springs. *Genome announcements*, *5*(40), pp.e00820-17.

Figure 1:

Location of Jinata Onsen on Shikinejima Island, Japan, and inset overview sketch of field site with sampling localities marked.

Figure 2:
Representative photos of Jinata. A) Panorama of field site, with Source Pool on the left (Pool 1 below), Pool 2 and 3 in the center, and Out Flow to the bay on the right. B) Undistorted view north up the canyon. C) Undistorted view south toward the bay, overlooking Pool 2. D) Source Pool, coated in floc-y iron oxides and bubbling with gas mixture containing H_2, CO_2, and CH_4. E) Pool 2, with mixture of red iron oxides and green from Cyanobacteria-rich microbial mats. F) Close up of textured microbial mats in Pool 3. G) Close up of Out Flow, where hot spring water mixes with ocean water.

Table 1: Geochemistry of source water at Jinata Onsen.

T	63°C
pH	5.4
DO	4.7 μM
Fe^{2+}	261 μM
NH_3/NH_4^+	87 μM
Cl^-	654 mM
SO_4^{--}	17 mM
NO_3^-	<1.6 μM
NO_2^-	<2.2 μM
HPO_4^-	<1 μM

Figure 3:
Summary of geochemical and microbiological trends along the flow path of Jinata Onsen. Top: panoramic view of Jinata Onsen, with Source Pool at left and flow of spring water toward the bay at right, with sampling locations indicated. Middle: geochemical transect across the spring, showing temperature (°C, left axis) and dissolved Fe(II) and O_2 (μM, right axis). Bottom: stacked bar chart of relative community abundance of dominant microbial phyla as determined by 16S rDNA amplicon sequencing. Sequence data were binned at the phylum level averaged at each sample site. Reads that could not be assigned to a phylum were discarded; all phyla that do not make up more than 2% of the community at any one site have been collapsed to "Other". Near the source, the community is predominantly made up of iron- and/or hydrogen-oxidizing organisms in the Proteobacteria and Aquificae phyla. As the hot spring water flows downstream, it equilibrates with the atmosphere and eventually mixes with seawater, resulting in downstream cooling, accumulation of oxygen, and loss of dissolved iron due to biological and abiotic processes. Oxygenic Cyanobacteria become progressively more abundant downstream Hydrogen- and iron-oxidizing lithotrophs dominate near the source, but phototrophic Cyanobacteria come to dominate downstream. Additional community diversity is found in Supplemental Table 4.

Figure 4:
Phylogeny of Bacteria and Archaea based on concatenated ribosomal proteins. Numbers in parentheses next to phylum labels refer to number of MAGs recovered from Jinata Onsen. Labels for phyla with two or fewer MAGs recovered from Jinata omitted for clarity. Reference alignment modified from (87). Full list of MAGs recovered available in Supplemental Table 6.

Figure 5: Phylogeny of the Zetaproteobacteria, rooted with Alphaproteobacteria, built with concatenated ribosomal protein sequences. Data from references 23, 89, 90, and other draft genomes available on Genbank. All nodes recovered TBE support values greater than 0.7. In cases where reference genomes have a unique strain name or identifier, this is included; otherwise Genbank WGS genome prefixes are used.

Figure 6: Phylogeny of the Calditrichaeota, rooted with Bacteroidetes, built with concatenated ribosomal protein sequences. Data from reference 91 and other draft genomes available on genomes have a unique strain name or identifier, this is included; otherwise Genbank WGS genome prefixes are used.

Figure 7: Detailed phylogeny of the Chloroflexi phylum, with class-level clades highlighted in gray, built with concatenated ribosomal protein sequences. The large basal class Dehalococcoidia, which was not observed in 16S rDNA or metagenome data from Jinata, is omitted for clarity. Contains MAGs reported here, members of the Chloroflexi phylum previously described (7, 38, 41, 92-104), and members of the closely related phylum Armatimonadetes as an outgroup (105, 106). MAGs described here highlighted in green, MAGs previously reported from Jinata Onsen highlighted in pink. All nodes recovered TBE support values greater than 0.7. In cases where reference genomes have a unique strain name or identifier, this is included; otherwise Genbank WGS genome prefixes are used.

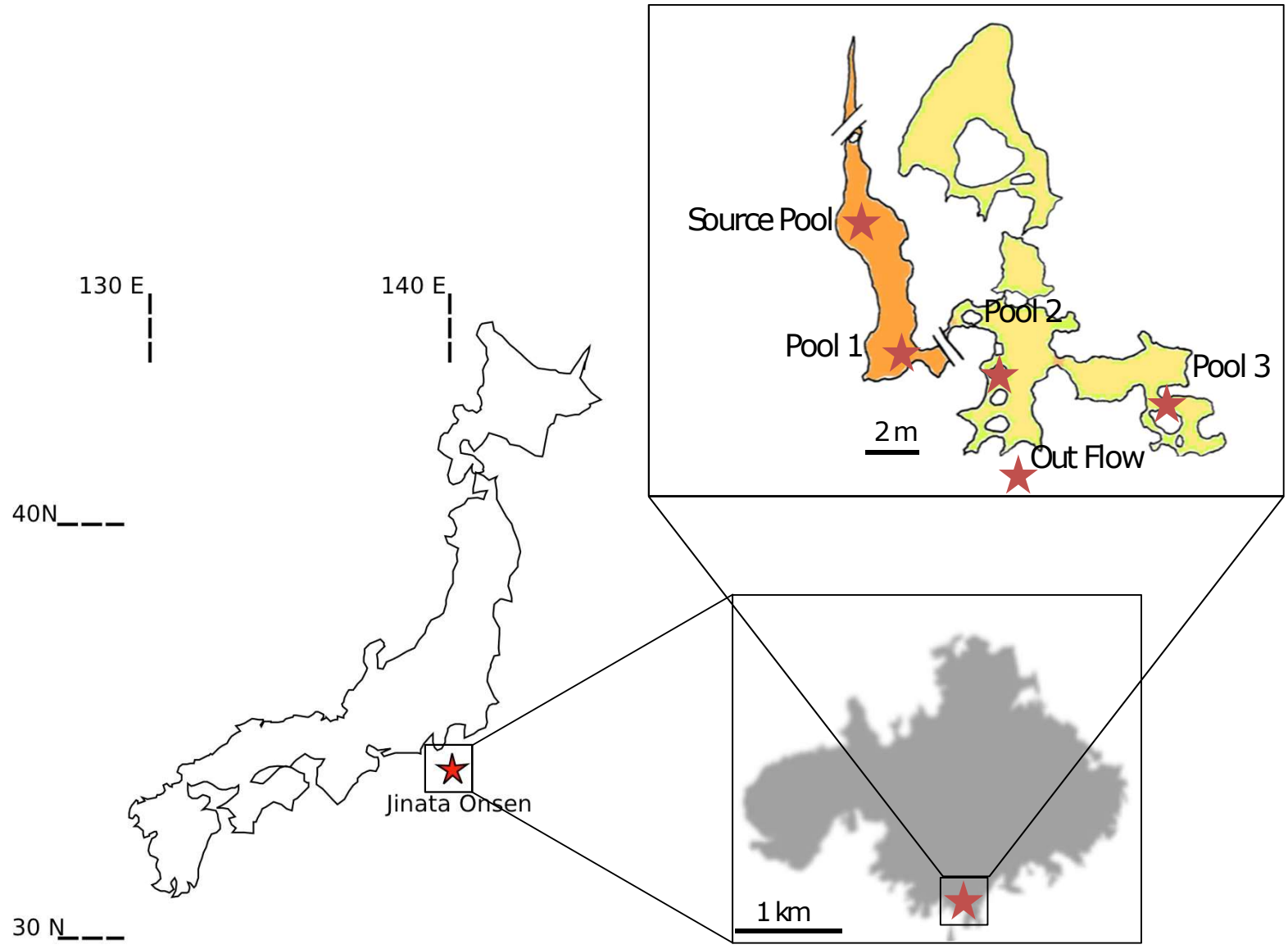
130 E
140 E
40N
30 N
Jinata Onsen
Source Pool
Pool 1
Pool 2
Pool 3
Out Flow
2 m
1 km


A)
B)
C)
D)
E)
F)
G)


Source
Pool 1
Pool 2
Pool 3
OutFlow

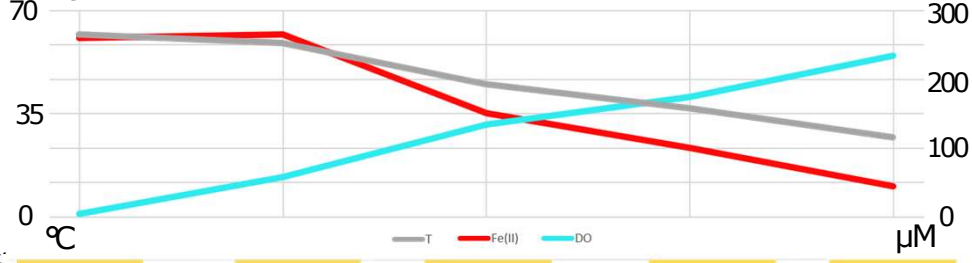
70
35
0
300
200
100
0
℃
μM
T
Fe(II)
DO

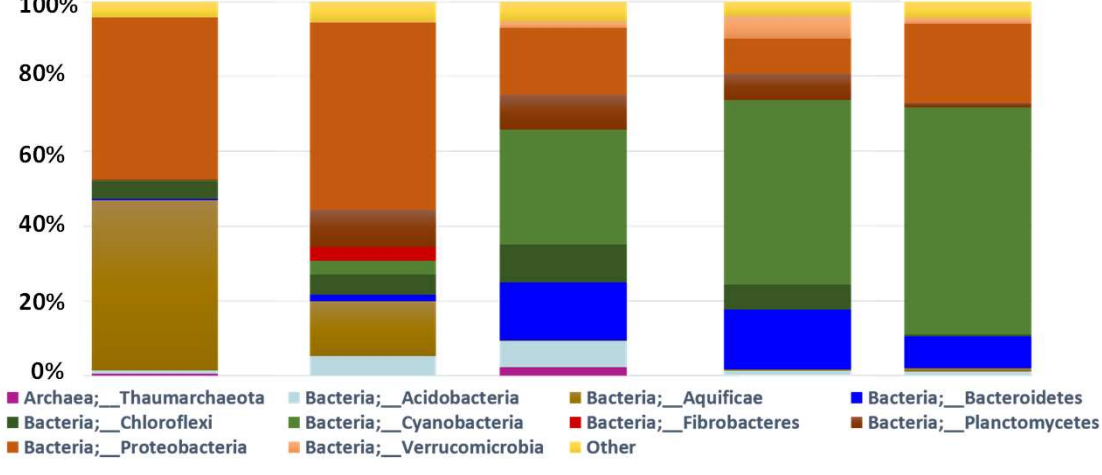
100%
80%
60%
40%
20%
0%
Archaea;__Thaumarchaeota
Bacteria;__Acidobacteria
Bacteria;__Aquificae
Bacteria;__Bacteroidetes
Bacteria;__Chloroflexi
Bacteria;__Cyanobacteria
Bacteria;__Fibrobacteres
Bacteria;__Planctomycetes
Bacteria;__Proteobacteria
Bacteria;__Verrucomicrobia
Other

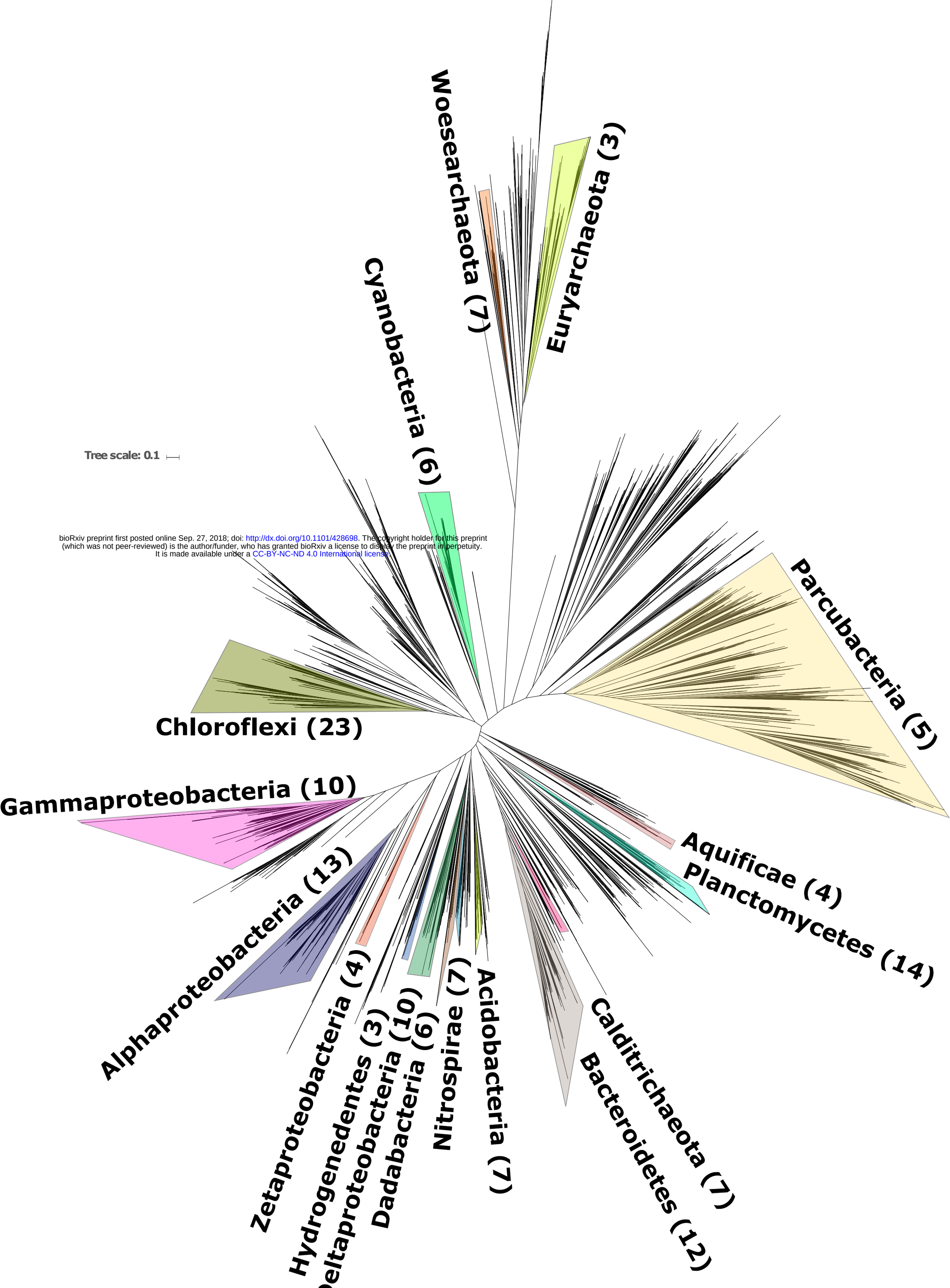

Tree scale: 0.1

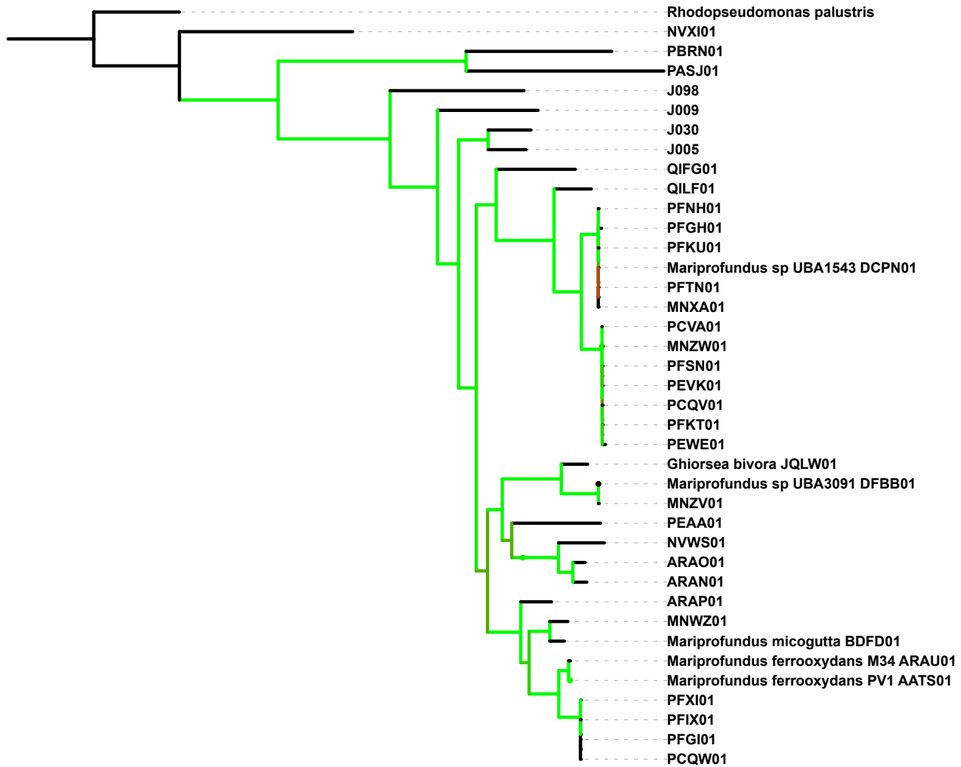

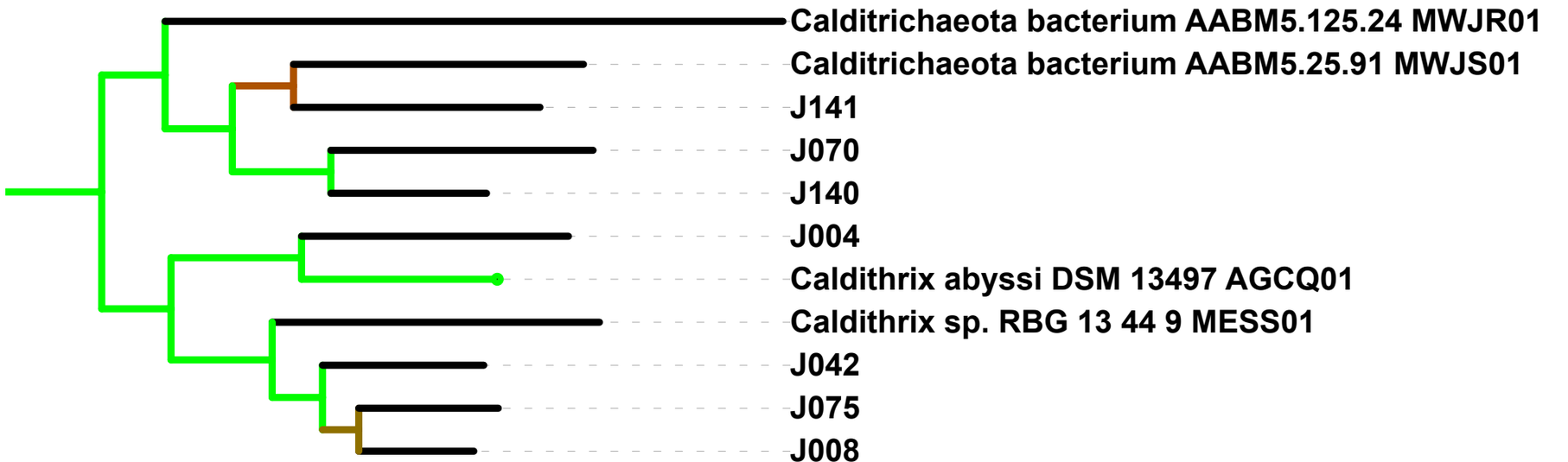
Calditrichaeota bacterium AABM5.125.24 MWJR01
Calditrichaeota bacterium AABM5.25.91 MWJS01
J141
J070
J140
J004
Caldithrix abyssi DSM 13497 AGCQ01
Caldithrix sp. RBG 13 44 9 MESS01
J042
J075
J008

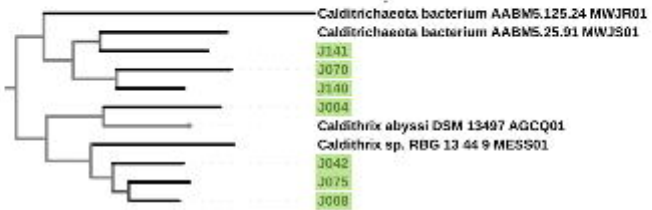
Calditrichaeota bacterium AABM5.125.24 MWJR01
Calditrichaeota bacterium AABM5.25.91 MWJS01
J141
J070
J140
J004
Caldithrix abyssi DSM 13497 AGCQ01
Caldithrix sp. RBG 13 44 9 MESS01
J042
J075
J008